Development 128, 3133-3144 (2001)
Printed in Great Britain © The Company of Biologists Limited 2001
DEV1686

Pax6 regulates granule cell polarization during parallel fiber formation in the developing cerebellum

Takao Yamasaki[1,2], Kousuke Kawaji[1,2], Katsuhiko Ono[3], Haruhiko Bito[4,5], Tomoo Hirano[1,2], Noriko Osumi[2,6] and Mineko Kengaku[1,2,*]

[1]Department of Biophysics, Graduate School of Science, Kyoto University, Sakyo-ku, Kyoto 606-8502, Japan
[2]CREST, Japan Science and Technology Corporation, Kawaguchi 332-0012, Japan
[3]Department of Anatomy, Shimane Medical University, Izumo 693-8501
[4]Department of Pharmacology, Faculty of Medicine, Kyoto University, Kyoto 606-8315
[5]TOREST, Japan Science and Technology Corporation, Kawaguchi 332-0012, Japan
[6]Department of Developmental Neurobiology, Tohoku Univeristy Graduate School of Medicine, Sendai 980-8575, Japan
*Author for correspondence (e-mail: kengaku@nb.biophys.kyoto-u.ac.jp

Accepted 14 May 2001

SUMMARY

The molecular mechanisms that govern the coordinated programs of axonogenesis and cell body migration of the cerebellar granule cell are not well understood. In *Pax6* mutant rats (*rSey²/rSey²*), granule cells in the external germinal layer (EGL) fail to form parallel fiber axons and to migrate tangentially along these fibers despite normal expression of differentiation markers. In culture, mutant cells sprout multiple neurites with enlarged growth cones, suggesting that the absence of *Pax6* function perturbs cytoskeletal organization. Some of these alterations are cell-autonomous and rescuable by ectopic expression of *Pax6* but not by co-culture with wild-type EGL cells. Cell-autonomous control of cytoskeletal dynamics by *Pax6* is independent of the ROCK-mediated Rho small GTPase pathway. We propose that in addition to its roles during early patterning of the CNS, *Pax6* is involved in a novel regulatory step of cytoskeletal organization during polarization and migration of CNS neurons.

Key words: Pax6, Cerebellum, Cell polarization, Granule cell, Parallel fiber, Cytoskeleton

INTRODUCTION

Neural circuitry of the vertebrate CNS develops through the coordinated program of neuronal migration, neurite outgrowth and synaptic interconnections between constituent neurons. The mammalian cerebellum provides a favorable system with which to study the formation of neural circuitry because of its relative simplicity and clear cytoarchitecture. Early steps that are crucial for the establishment of synaptic connectivity in the cerebellar cortex are axon formation and dynamic migration of granule cell neurons (Hatten and Heintz, 1995; Altman and Bayer, 1997). Granule cells are generated in the external germinal layer (EGL), which covers the outer surface of the cerebellar cortex. Then, postmitotic neurons in the deep EGL extend bipolar axons horizontally to the pial surface, and subsequently move their cell bodies along the axis of the developing axons. During postnatal development, granule cells extrude a third process inwardly and make a 90° turn to descend into the internal granular layer (IGL). Migrating neurons leave trailing processes attached to the horizontal beams of the bipolar axons, forming the characteristic T-shaped axons, the parallel fibers. These parallel fibers ultimately innervate the Purkinje cells, the principal neurons of the cerebellar cortex.

A variety of molecules are known to act during axon formation and migration (Goodman and Shatz, 1993; Goodhill, 1998). These include long-range and short-range guidance molecules, signaling molecules that interpret and decode these cues, and cytoskeletal components that regulate cell morphology. Several signaling molecules, including ROCK (Bito et al., 2000), Unc51.1 (Tomoda et al., 1999) and DDR1 (Bhatt et al., 2000), have been implicated in the early steps of axonogenesis of granule cells in vitro. ROCK is a serine/threonine kinase activated downstream of Rho GTPase. Intensive studies have elucidated the importance of regulation by Rho family small GTPases in cytoskeletal reorganization during neuronal morphogenesis and migration (Luo et al., 1996; Threadgill et al., 1997; Zipkin et al., 1997; Steven et al., 1998; Albertinazzi et al., 1999; Nakayama et al., 2000). Inhibition of ROCK activity in cultured granule cells triggers excessive sprouting of axons, suggesting that the Rho/ROCK pathway negatively controls axon outgrowth probably through organizing actin dynamics, especially during the initial step of polarity induction (Bradke and Dotti, 1999; Bito et al., 2000). However, Unc51.1 and DDR1 have been shown to act as positive regulators of axon outgrowth as revealed by dominant-negative inhibition of these molecules (Tomoda et al., 1999; Bhatt et al., 2000). It remains elusive, however, how the

activities of these molecules are orchestrated during cellular morphogenesis of the granule cell.

Differentiation of granule cells is thought to depend on both genetic programs intrinsic to the granule cells and epigenetic influences of adjacent siblings as well as of other cell types in the developing cerebellum (Trenkner et al., 1984; Dahmane and Ruiz-i-Altaba, 1999; Wechsler-Reya and Scott, 1999). Studies using culture systems have demonstrated that granule cells autonomously develop polarity to form parallel fibers in the absence of spatial cues (Nagata and Nakatsuji, 1991; Powell et al., 1997). One candidate molecule implicated in such an intrinsic mechanism is a paired domain-containing homeobox gene, *Pax6*. In the *Pax6* mutant mouse, small eye (*Sey/Sey*), the EGL is malformed and the horizontal array of newly forming parallel fibers is disorganized (Engelkamp et al., 1999). Besides this anomaly in the EGL, multiple neurological defects are also seen in the mutant cerebellum, including attenuated foliation, misplacement of a subset of EGL cells and deformity in the vermis-forming territory (Engelkamp et al., 1999). It remains unknown which of these defects are direct or indirect consequences of lack of *Pax6* function.

Pax6 is known as a morphogenetic gene with a myriad of activities in patterning (Stoykova et al., 2000; Toresson et al., 2000; Yun et al., 2001) and cell-type specification (Burrill et al., 1997; Ericson et al., 1997; Osumi et al., 1997) during early development of the CNS. It has also been shown that *Pax6* is involved in various aspects of axon pathfinding and migration of CNS neurons. These include radial migration of cortical neurons (Schmahl et al., 1993; Caric et al., 1997), formation of thalamo-cortical projections (Kawano et al., 1999; Pratt et al., 2000), and formation of longitudinal and medial-ventral tracts in the forebrain (Mastick et al., 1997; Vitalis et al., 2000). However, disruption of these processes in the *Pax6* mutant CNS appears to be an indirect consequence of the loss of a prerequisite role of *Pax6* in conferring regional identity to the neurons, which either express *Pax6* or interact with *Pax6*-expressing cells. In the forebrain, for example, *Pax6* expression defines the midbrain-forebrain boundary and provides local guidance information to the post-optic commissure axons (Mastick et al., 1997).

In this study, we present evidence for a novel role for *Pax6* as a critical regulator in cell polarization in the cerebellar granule cell. *Pax6* mutation caused severe deficits in initial polarization of axons and the cytoskeletal reorganization in growth cones. Furthermore, cell body migration was aberrant in *Pax6* mutant granule cells. These phenotypes appeared to be due to the absence of intrinsic activity of *Pax6* in the granule cell. It is thus suggested that *Pax6*-mediated transcriptional control is essential to achieve proper granule cell polarization during parallel fiber formation both in vivo and in vitro.

MATERIALS AND METHODS

Animals

small eye rats (*rSey*^{2} allele on a Sprague-Dawley (SD) background; Osumi et al., 1997) were maintained in laboratory colonies at the National Center for Neurology and Psychiatry and Tohoku University Graduate School of Medicine. Homozygous embryos derived from intercrosses of *rSey*^{2}/+ were distinguishable by their external morphology. Wild-type embryos were obtained from intercrosses of heterozygous or of wild-type SD rats. The day of vaginal plug was considered as E0.

Microexplant and reaggregate cultures

Microexplant cultures of wild-type and *rSey*^{2}/*rSey*^{2}EGL at E21 were prepared as described by Nagata and Nakatsuji (Nagata and Nakatsuji, 1991). Reaggregate cultures were basically performed as described (Nagata and Nakatsuji, 1994). Briefly, the EGLs from E21 wild-type and *rSey*^{2}/*rSey*^{2} embryos were dissociated, and fractions containing small neurons were collected and labeled with PKH26 (Sigma). Unlabeled host cells were prepared from P2 EGL and mixed with labeled cells at a ratio of 20:1. The cell mixture was centrifuged in an Eppendorf tube and incubated for 1 hour to make reaggregates that were then cut into 300-400 μm pieces and placed on culture dishes coated with poly-D-lysine/laminin. Cultures were maintained at 37°C in 5% CO_2 and analyzed after 1-3 days.

Immunohistochemistry and fluorescent microscopy

Cultures and fresh-frozen cryosections (10 μm) were fixed with 4% paraformaldehyde (PFA) for 15 minutes at room temperature. Primary and secondary antibodies used for staining were as follows: mouse monoclonal antibody (mAb) against TAG-1 (4D7; 1:4, DSHB); mAb against Zic1 (1:50, kindly provided by J. Aruga); mAb against MAP2 (1:200, Sigma); mAb against Tau1 (1:200, Boehringer Manheim); mAb against α-tubulin (1:200, Sigma); rabbit polyclonal antibody (pAb) against Pax6 (Inoue et al., 2000); pAb against 440-kD Ankyrin$_B$ (1:200, kindly provided by M. Kunimoto); and goat anti-rabbit or anti-mouse secondary antibodies conjugated with FITC, AMCA (Chemicon) or Alexa568 (Molecular Probes). F-actin was stained with Oregon Green 488-phalloidin (1:100, Molecular Probes). After washing, slides were mounted in a glycerol-based medium SlowFade (Molecular Probes) and analyzed using a Nikon E800 microscope with ×20 and ×40 PlanFluor objectives.

For quantitative analysis of the number and length of axons, the trace from the contour limit of the cell soma to the tip of the major process of the neuron was defined as its axon length. Processes longer than 3 μm emerging from the soma, or those longer than 10 μm bifurcating from the shaft were counted as axons. To quantify the relative size of the growth cones, live cells labeled with PKH26 were kept at 37°C and observed using water-immersed 40× Fluor objective (0.80W). The size of growth cones was measured using the graphic image of IpLab (Scananalytic).

DiI labeling of EGL cells

E21 cerebella fixed with 4% paraformaldehyde (PFA) were embedded in 3% agar and cut coronally at a thickness of 200 μm using a vibratome. Small crystals of the lipophilic dye DiI were placed on the EGL and left for 10 days at 4°C to allow diffusion of the dye. After washing away the crystals, sections were mounted and analyzed using a fluorescent microscope.

Transmission and scanning electron microscopies (TEM and SEM)

Cultured cells were fixed with 4% PFA and 5% glutaraldehyde in phosphate buffer (PB; 0.1M, pH 7.4) at room temperature overnight. They were washed with PB and post-fixed with 1% osmium tetroxide in PB for 1 hour. For TEM, the samples were washed well with distilled water (DW) and stained en bloc with 1% uranyl acetate for 1 hour. They were then dehydrated through a graded ethanol series, cleared with hydroxypropyl metacrylate and embedded in Epon 812. They were cut with a ultramicrotome and observed under an TEM (JEM-1200EX, JEOL; or EM-002B, Topcon, Japan) at an accelerating voltage of 80 kV. For SEM, the samples washed with DW were subsequently immersed in 2% tannic acid for 1 hour, and then 1% osmium tetroxide in DW for 1 hour (Katsumoto et al., 1981). They were dehydrated and immersed in *t*-butyl alcohol. The samples were

dried at critical point (JFD-300, JEOL, Japan), coated with platinum/palladium and observed under an SEM (H-800, Hitachi, Japan) at an accelerating voltage of 15 kV.

In situ hybridization

In situ hybridization on cryosections was performed by a method described previously (Lin and Cepko, 1998). The rat Pax6 cDNA used as a probe was described previously (Matsuo et al., 1993).

Transfection of plasmid cDNA

Plasmid cDNAs used for transfection were as follows: mouse Pax6 and Pax6-EnR cDNAs subcloned in a pCAX expression vector (full-length cDNA of mouse Pax6 was kindly provided by P. Gruss); ROCK-Delta3 (Ishizaki et al., 1997); C3-GFP (Watanabe et al., 1999); and EGFP-N1 (Clontech).

For expression in a microexplant culture, a modified calcium phosphate procedure developed by A. Ghosh was used (Threadgill et al., 1997). Transfections were performed 6-12 hours after plating when emigrating cells were observed. Plasmids used were either 2 μg GFP-N1 alone or a mixture of 0.8 μg GFP-N1 and 2.4 μg plasmid of interest per well on multi-well plates (Nunclon Multidish four wells, Nunc). Analysis was carried out 24-36 hours after transfection. Under these conditions, usually 10-40 neurons expressed GFP. The efficacy of co-transfection was >80%.

Transfections in low-density cultures of dissociated cells were performed as previously described (Bito et al., 2000). Small cerebellar neurons were labeled with PKH26 and plated at 2×10^5 cells per well in polylysine/laminin-coated wells. Cells were fixed 20 hours after transfection for fluorescent microscopy. Some cells were stained with F-actin or with anti-Tau instead of PKH26, all of which gave basically the same results.

Construction and infection of recombinant retrovirus

The Pax6-EnR chimera was created by fusing the N-terminal domain of Pax6, which contains two DNA binding sites (amino acids 3-306), with the Engrailed repressor domain. Using PCR-based mutagenesis, *Nco*I and *Eco*RI sites were introduced in the Pax6 cDNA at the first methionine and at the amino acids 307-308, respectively. Primers used were as follows; 5′-GACTCGAGCCATGGAGAACAGTCACA-GCGG-3′, 5′-CTGATATCGACAGGTGTGGT-GGGCTG-3′. The *Nco*I-*Eco*RV fragment of the PCR product was ligated into a pBluescript IISK+. The insert was cut with *Nco*I and *Eco*RI and then ligated into a *Nco*I-*Eco*RI-digested EnR-pSLAX21 (kindly provided by T. Furukawa). The entire Pax6-EnR fusion and EnR were cloned into a retroviral vector pLIA as described by Furukawa et al. (Furukawa et al., 1997). The viruses were produced in a Phoenix cell line (generously provided by G. Nolan), and were concentrated at 1×10^6-1×10^8 pfu/ml according to the procedure described by Cepko (Cepko, 1998).

To inject virus, neonatal ICR mice were anesthetized on ice. A Hamilton microliter syringe (Hamilton, Whitter, CA) was inserted through the skin and the skull to a position above the EGL and 1 μl of virus solution was injected over 2 minutes. The pups were revived at 36°C and returned to the litter. At 10 days post-transfection, infected cerebella were dissected, sectioned at 50 μm using vibratome and stained for AP.

RESULTS

Parallel fiber formation is disrupted in the *Pax6* mutant cerebellum

Granule cell progenitors form the EGL by the end of gestation. During postnatal development, the EGL is subdivided into two sublayers; the granule cell progenitors continue mitosis in the outer sublayer, whereas postmitotic neurons start to extend bipolar axons and move horizontally in the inner sublayer of the EGL (Hatten and Heintz, 1995; Altman and Bayer, 1997). Previous studies have documented that, while proliferation remained unaffected, the postmitotic granule cells fail to segregate in the inner premigratory layer of the EGL in the *Pax6* mutant mice small eye (*Sey/Sey;* Engelkamp et al., 1999).

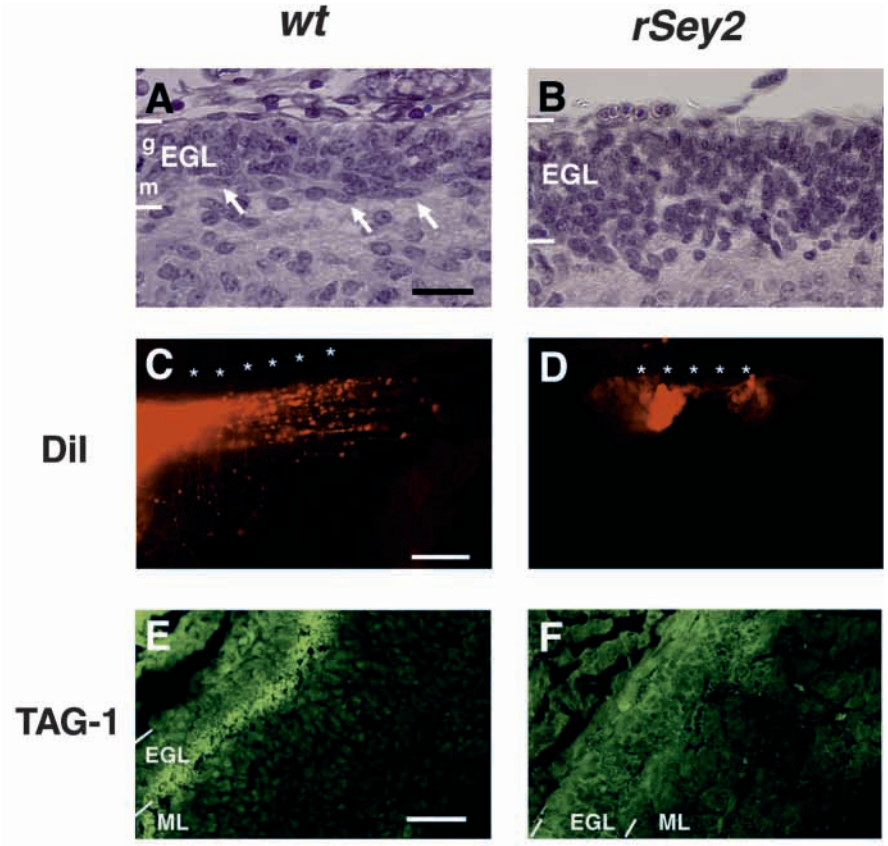

Fig. 1. Disrupted formation of the EGL and the parallel fibers in *Pax6* mutant (*rSey*^{2}/*rSey*^{2}) cerebella. (A,B) HE-stained cross-sections of E21 cerebella. The wild-type EGL (A) is subdivided in the outer germinal layer (g) and the inner premigratory layer (m). Spindle-shaped cells (arrows) in the premigratory layer are presumably migrating along the young parallel fibers. *Pax6* mutant EGL (B) is thicker and uniform accumulation of round cells is observed. (C,D) DiI-labeled parallel fibers. Horizontal beams of parallel fibers in the deep EGL of the wild-type cerebellum (C) are not formed in the *Pax6* mutant (D). Pial surface of the cerebella is indicated by asterisks. (E,F) Expression of TAG-1 in E21 cerebella. TAG-1 signal delineates the boundary between the EGL and the molecular layer in the wild-type cerebellum (E). TAG-1 is diffusely expressed throughout the EGL in the *Pax6* mutant cerebellum (F). Some background autofluorescence can be observed in the vascular cells on the pial surface of the EGL. Scale bars: 25 μm in A-D; 40 μm in E,F.

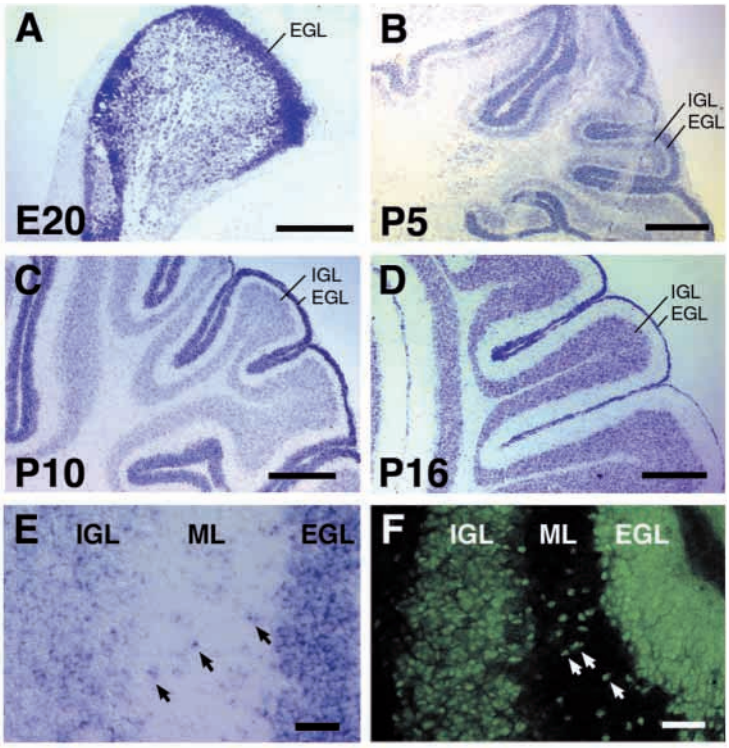

Fig. 2. *Pax6* expression in differentiating granule cells during development. (A-D) In situ hybridization with a Pax6 probe was performed on sagittal cryosections of developing rat cerebella of E20 and postnatal days 5, 10 and 16. *Pax6* is continuously expressed in developing granule cells in the EGL and the IGL. (E) Higher magnification of P10 cerebellum. Expression is stronger in the EGL than in the IGL. Some cells in the ML also express *Pax6* mRNA (arrows). (F) Immunohistochemistry of P10 cerebellum for Pax6 protein reveals intense expression in the EGL and in migrating granule cells with fusiform nuclei in the ML (arrows); expression in the IGL is relatively weak. Scale bars: 250 μm in A-D; 25 μm in E,F.

Using a *Pax6* mutant rat *rSey²/rSey²* (Osumi et al., 1997), we confirmed that this phenotype was a general feature of *Pax6*-deficiency (Fig. 1A,B). We next analyzed the formation of parallel fibers in the wild-type and the mutant cerebella by DiI labeling and immunofluorescent studies. In the E21 wild-type rat, DiI particles implanted in the EGL labeled multiple long neurites aligned parallel to the pial surface in the deeper portion of the EGL (Fig. 1C). The deep EGL was also delineated by expression of TAG-1, a transient marker for early parallel fibers (Fig. 1E; Furley et al., 1990; Yamamoto et al., 1990). These data suggest that the postmitotic EGL cells are already forming the premigratory layer and extending parallel fibers by late gestation. In contrast, DiI incorporation by several round EGL cells resulted in labeling of very few neurites in the *rSey²/rSey²* EGL (Fig. 1D). Additionally, TAG-1-positive cells were randomly dispersed in the *rSey²/rSey²* EGL and never observed to form a sharp band, as seen in the wild-type cerebellum (Fig. 1E,F). These results indicate that the EGL cells of *Pax6* mutants fail to form the premigratory layer and to extend the parallel fibers, in accordance with the previous study (Engelkamp et al., 1999).

Pax6 is expressed in the granule cells during development

To explore *Pax6* activity during granule cell differentiation, we examined *Pax6* expression in developing rat cerebella. *Pax6* transcripts were detected in the EGL throughout pre- and postnatal development (Fig. 2A-D). At E20, intense expression of *Pax6* mRNA was observed in the EGL cells and in dispersed cells in the cerebellar cortical primordia (Fig. 2A). After P5, *Pax6* expression was seen in postmigratory granule cells in the emerging IGL at reduced levels compared with premigratory EGL cells (Fig. 2B-D; Stoykova and Gruss, 1994). Observation at higher magnification revealed that a subset of cells in the molecular layer (ML) also expressed *Pax6* mRNA (arrows in Fig. 2E). Expression of Pax6 protein showed basically the same profile (Fig. 2F); immunoreactivity was prominent in the EGL cells and declined in the IGL cells. Cells in the ML that expressed Pax6 protein had fusiform nuclei, suggesting that they were granule cells migrating from the EGL to the IGL. Thus, *Pax6* mRNA and protein are expressed in granule cells throughout the course of their differentiation and migration.

Pax6 mutant cells differentiate as granule cells but fail to form bipolar axons and migrate in random orientation

The expression pattern of *Pax6* in developing cerebella prompted us to examine its potential role during neurite outgrowth and migration of granule cells. As the homozygous mutants die at birth during the early phase of granule cell differentiation, we performed microexplant cultures of E21 EGL in which cell-autonomous migration and cellular morphogenesis of the granule cells can be reconstituted (Nagata and Nakatsuji, 1991). By 1 day in culture (1 DIV), wild-type cells extruded long neurites radially and emigrated out from the EGL explant. The radial neurites formed parallel bundles after 2 DIV. TEM and time-lapse tracing showed that most neurons maintained close contact with the bundles of preexisting long neurites and migrated along straight trajectories (Fig. 3A,C). In contrast, only a few radial fibers were seen in the *Pax6* mutant EGL culture. TEM revealed that many round cells failed to form long leading processes in the mutant cultures (Fig. 3B). Active migration was observed, although the cells dispersed randomly (Fig. 3D). The radial migration of cultured granule cells has been shown to be dependent on laminin substrate (Nagata and Nakatsuji, 1990). We therefore checked the expression of putative binding partners of laminin in granule cells, L1 and β1-integrin. Both are expressed equally in wild-type and mutant cells, precluding the possibility that the disorganized appearance of *Pax6* mutant cells was due to mere non-responsiveness to laminin substrate (data not shown).

The morphology and behavior of the mutant cells raised the possibility that differentiation of the granule cells might be disturbed or delayed in the absence of *Pax6* expression. To test this, we examined the expression of several neuronal and granule cell markers by immunofluorescence. We first confirmed that 70-80% of emigrating cells from the wild-type and mutant explants were granule cells and/or granule cell progenitors, as revealed by Zic1 expression (data not shown; Aruga et al., 1994). These cells strongly expressed Pax6

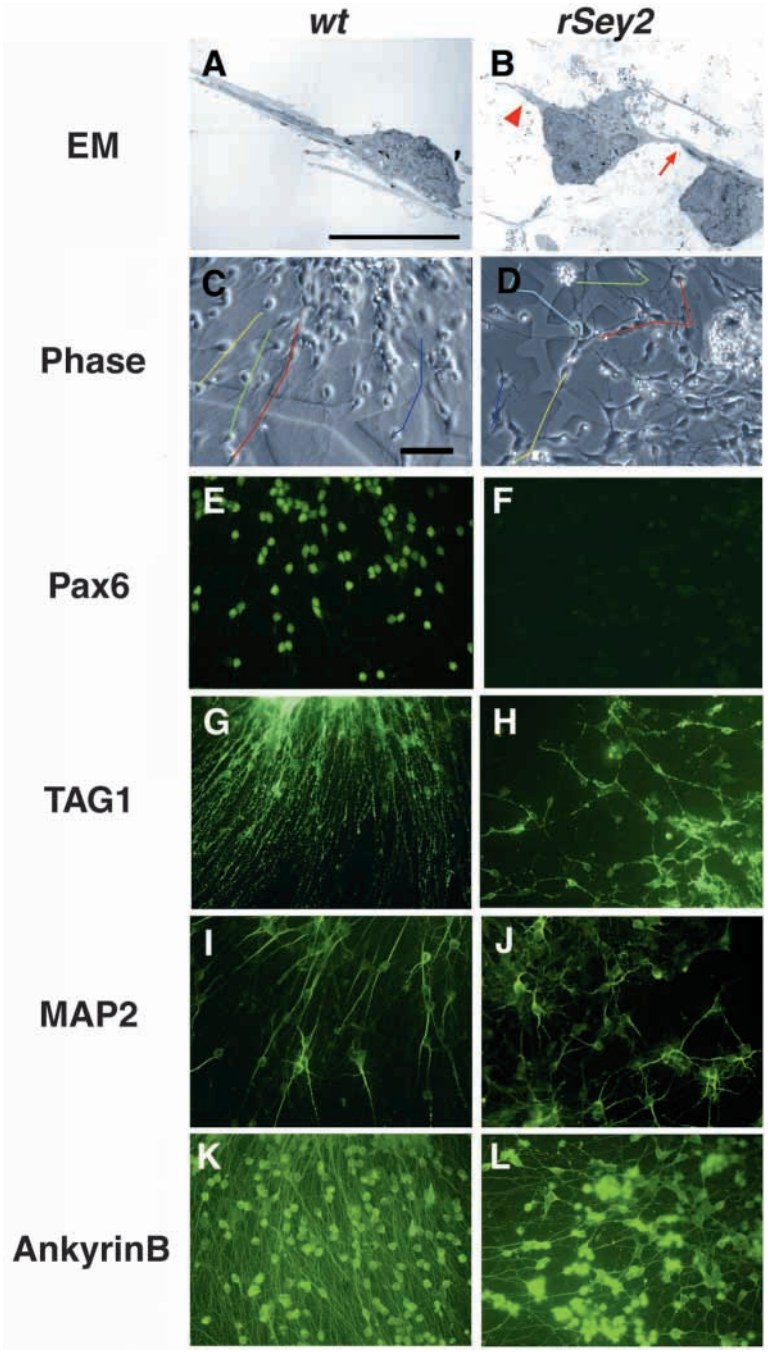

Fig. 3. Abnormal morphology and migration of granule cells in microexplant cultures of the *Pax6* mutant (*rSey*^{2}/*rSey*^{2}) EGL. (A,B) Transmission electron micrographs of the EGL cells in culture (3 DIV). Spindle-shaped granule cell has long, thick leading process associated with preformed neurites of other cells in the wild-type culture (A). *Pax6* mutant cells are round in morphology and form short thin processes attached to (arrow) or detached from (arrowhead) neighboring cells (B). (C,D) Phase-contrast light micrographs of EGL cells migrating from the explant (2 DIV). Colored lines are trajectories of the granule cells traced for 8 hours. While wild-type cells extend long radial neurites and migrate along the fibers (C), *Pax6* mutant cells lack long neurites and move randomly (D). (E,F) Pax6 expression. (G,H) TAG-1 expression. Wild-type cells extend TAG-1-positive long neurites (G), while mutant cells express TAG-1 around their cell bodies and in the short neurites (H). (I,J) MAP2 expression demarcates the leading processes of migrating neurons. (K,L) Differentiation of parallel fibers is shown by 440 kDa Ankyrin$_B$-positive staining in wild-type cells (K). *Pax6* mutant cells express Ankyrin$_B$ in irregularly aligned processes (L). Cultures were maintained for 40 hours (E-J) and 72 hours (K,L). Scale bars: 10 μm in A,B; 50 μm in C-L.

protein in wild-type cultures, while no Pax6 antigen was detectable in mutant cultures (Fig. 3E,F). A subset of cells that emigrated from the wild-type explant expressed TAG-1, an early marker for parallel fiber axons, on their long bipolar neurites (Fig. 3G). In contrast, although equal numbers of *Pax6* mutant cells showed strong expression of TAG-1 around their cell bodies, extension of TAG-1-positive long neurites was rarely seen (Fig. 3H). The expression of the microtubule-associated protein, MAP2, was mostly confined to the leading processes at 2 DIV in both wild-type and mutant explants (Ono et al., 1994). While wild-type cells regularly aligned long leading processes distally to the explant, mutant cells randomly misoriented short processes regardless of the orientation of other cells (Fig. 3I,J). *Pax6* mutant cells occasionally had multiple processes that expressed MAP2, suggesting an abnormal control of the leading process formation. After 3 DIV, many cells in both the wild-type and the mutant cultures had ceased expressing TAG-1, suggesting they had exited the early phase of granule cell differentiation (data not shown). These cells indeed strongly expressed 440 kDa Ankyrin$_B$, a specific marker for the parallel fiber axons (Kunimoto, 1995), together with Tau1, a general marker for axons (Fig. 3K,L and data not shown). In the wild-type culture, the massive radial neurites appeared to differentiate into Ankyrin$_B$-positive parallel fibers. *Pax6* mutant cells also synthesized Ankyrin$_B$ but formed large meshes of irregular neurites rather than organized parallel bundles. Little difference was observed in the relative numbers of GFAP-positive glia, most of which were found in close proximity to the explant, between the wild-type and the mutant cultures (around 10%; data not shown). After 3 DIV, we observed apoptotic cell death more frequently in mutant cultures, although it affected neither the apparent density nor the total number of surviving cells (data not shown). Taken together, these results suggest that *Pax6* mutant cells can recapitulate the typical cascade of gene expression during granule cell differentiation, but fail in correctly polarizing their parallel fiber axons and subsequently migrate in a disorganized manner.

Pax6 regulates morphogenesis and migration of granule cells in a cell-autonomous manner.

The specific expression of *Pax6* in developing granule cells suggests that abnormal polarization of *rSey*^{2}/*rSey*^{2} granule cells might be a direct consequence of loss of intrinsic *Pax6* activity within the differentiating granule cells. Alternatively, it may indicate that *Pax6* is involved in cell-cell interaction of granule cells with the same and/or other cell types in the cerebellum. To distinguish between these possibilities, we created a mixed culture of *rSey*^{2}/*rSey*^{2} mutant EGL cells with wild-type cells.

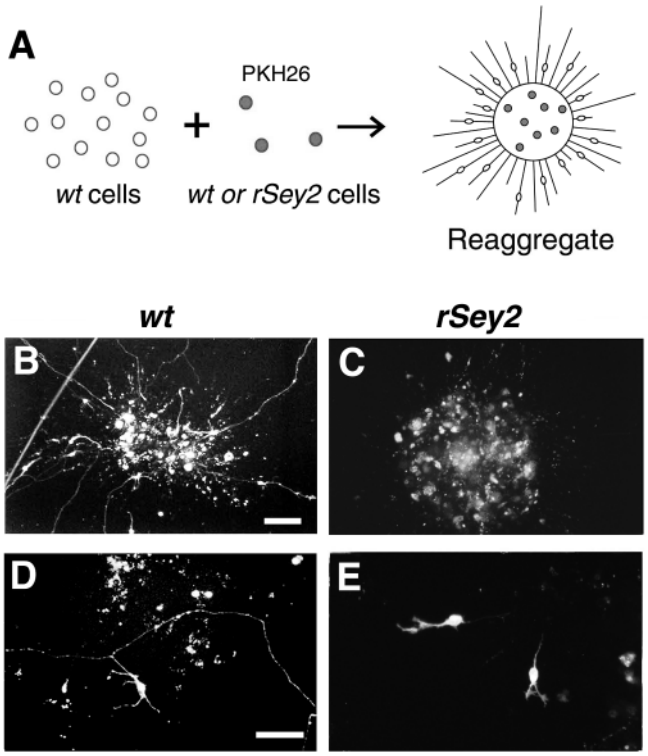

Fig. 4. Abnormal elongation and migration of *Pax6* mutant (*rSey*^{2}/*rSey*^{2}) EGL cells co-cultured with wild-type cells. (A) PKH26-labeled wild-type and *Pax6* mutant EGL cells from E21 embryos were mixed with P2 wild-type EGL cells at a ratio of 1:20 and cultured in cellular reaggregates. (B,D) Wild-type cells elongate long axons (B), which occasionally display T-shaped morphology (D). (C,E) Mutant cells rarely extend long neurites (C), often forming randomly misoriented dwarfed processes (E). Cultures were maintained for 40 hours (B,C) and 72 hours (D,E), respectively. Scale bars: 40 μm in B,C; 20 μm in D,E.

Cellular morphology was visualized by labeling cells with a fluorescent membrane-soluble dye PKH26 (Fig. 4A). The control wild-type cells labeled with PKH26 extended long neurites and migrated radially along the fibers (Fig. 4B). We occasionally observed cells with characteristic T-shaped axons resulting from vertical reorientation (Fig. 4D). On the other hand, *Pax6* mutant cells rarely elongated long neurites and scattered randomly in spite of the regular radial fibers formed by surrounding wild-type cells (Fig. 4C,E). These results suggest that the abnormal morphology and migration of *Pax6* mutant cells are cell-autonomous, as they could not be rescued by co-culture with wild-type cells.

To assess whether *Pax6* activity is sufficient to correct the anomalies of the mutant cells, we transfected *Pax6* cDNA into mutant cells. The number and the length of neurites of Zic1-positive cells were quantified by co-transfecting green fluorescent protein (GFP) cDNA in explant cultures (Fig. 5). When GFP cDNA was transfected alone, the proportion of Zic1-positive cells with longer neurites was significantly higher in wild-type cells than in mutant cells. Notably, we found a considerable number of neurons with more than two neurites in mutant cultures. In contrast, expression of *Pax6* in mutant cells restored wild-type phenotypes; most of the cells co-transfected with *Pax6* and GFP cDNAs became bipolar and extended neurites to lengths comparable with wild-type cells.

These results strongly suggest that *Pax6* functions intrinsically in the granule cell upstream of the formation of long bipolar neurites and orderly migration. To verify that *Pax6* function is truly involved in the genetic cascade of granule cell differentiation in normal developing cerebellum, we misexpressed a dominant-negative form of *Pax6* in granule cell precursors in situ as well as in vitro. The DNA-binding domain of *Pax6* was fused to the repressor domain of *Drosophila Engrailed* (*EnR*), producing a fusion protein that should block transcriptional activation by intrinsic *Pax6* (Furukawa et al., 1997; Matsunaga et al., 2000). We first confirmed that misexpression of the *Pax6-EnR* cDNA in the microexplant culture of wild-type cells resulted in multipolar morphology similar to *rSey*^{2}/*rSey*^{2} cells (Fig. 5). Thus, perturbation in the maintenance of *Pax6* function to activate transcription of the downstream target gene(s) was sufficient to cause the morphological deficits observed in *Pax6* mutant EGL cells even within the wild-type genetic background.

By utilizing a replication-incompetent retrovirus vector (pLIA), we next misexpressed the dominant-negative gene in neonatal EGL cells and assayed morphology and location of the infected cells after 10 days by staining for the marker gene AP (Fig. 6). During postnatal development, granule cell precursors represent almost the sole mitotic cells in the EGL infectable by retrovirus (Zhang and Goldman, 1996). Granule cell progenitors infected with control vector viruses or those carrying Engrailed repressor domain alone differentiated normally and correctly migrated to the IGL (Fig. 6B,F). They elongated bipolar parallel fibers in the molecular layer, formed glomeruli at the tip of dendrites and adopted a T-shape morphology, as visualized by AP staining (Fig. 6D). By contrast, most of the cells infected with viruses transducing the *Pax6-EnR* transgene remained in the EGL (Fig. 6C,F). Short, bushy processes were observed around their cell bodies in the EGL and few or no parallel fibers were formed in the ML (Fig. 6E). While descendant cells carrying the control viruses spread out over a broad area, those misexpressing Pax6-EnR tended to remain clustered around the injection site, possibly owing to the failure in tangential migration of the EGL cells in the absence of the leading process formation. It was also notable that a significantly smaller number of infected cells were observed with Pax6-EnR viruses, suggesting that *Pax6* might also contribute towards maintaining survival of granule cells during differentiation.

Taken together, these results indicate that *Pax6* functions as an intrinsic factor required for elongation of bipolar axons and subsequent orderly migration of granule cells in the developing EGL.

Aberrant sprouting of axons accompanies enlargement of growth cones in the *Pax6* mutant granule cells

The next obvious question was which step of cellular morphogenesis and migration was disturbed in the *Pax6* mutant granule cells. As shown in Fig. 3, *Pax6* mutant EGL cells expressed a series of differentiation markers, precluding the possibility that the onset of molecular switches in granule cell differentiation was simply retarded in the absence of *Pax6* function. Taking into account that Pax6 is a transcription factor,

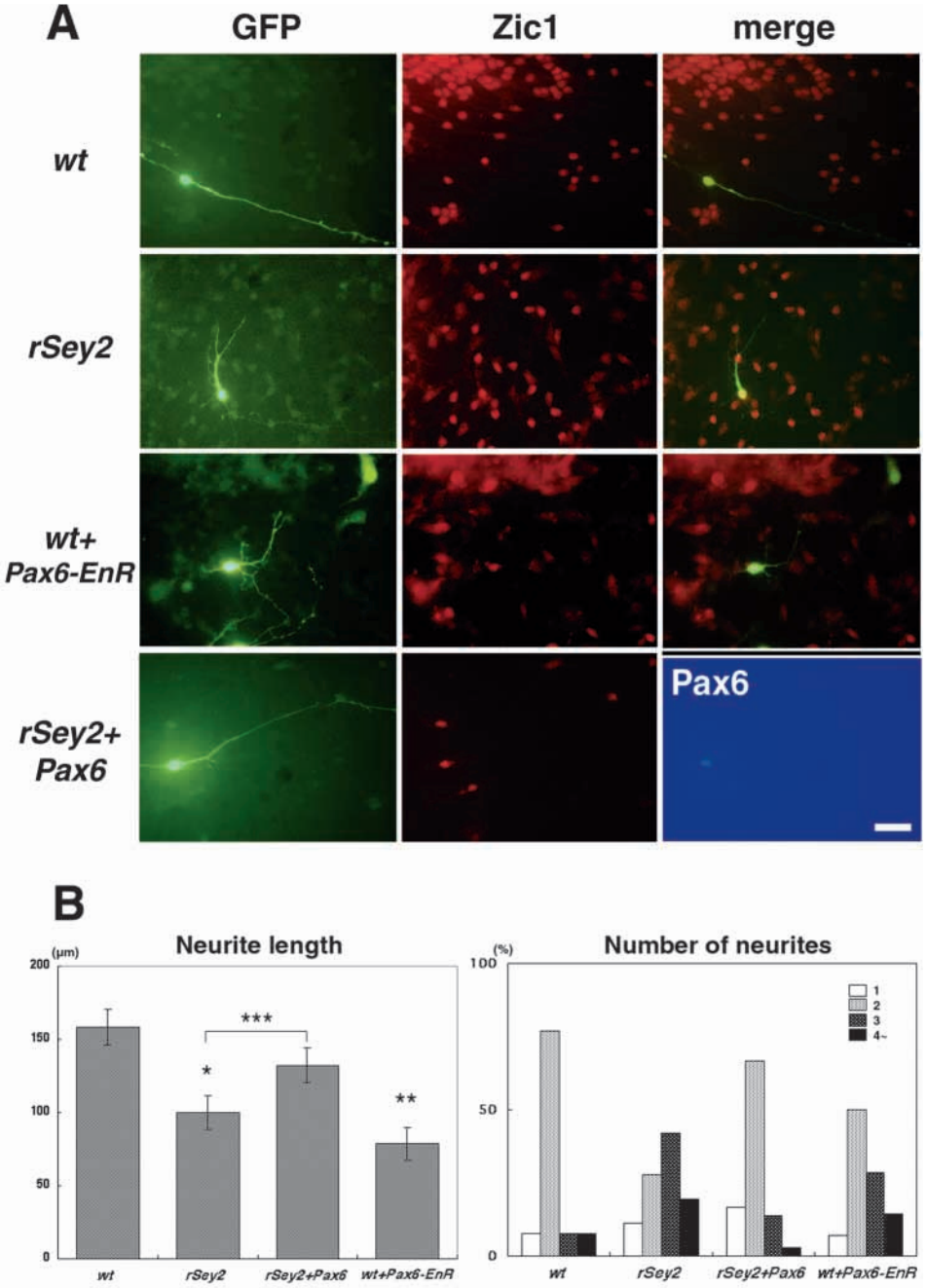

Fig. 5. Cell-autonomous effect of *Pax6* on elongation of bipolar parallel fibers. EGL cells in microexplant cultures were transfected with either GFP cDNA alone (*wt*, *rSey2*) or GFP with Pax6 or Pax6-EnR cDNAs (*rSey2+Pax6*, *wt+Pax6-EnR*). (A) Morphology of granule cells shown by GFP fluorescence (green) together with immunofluorescence with Zic1 (red) and Pax6 (blue). Scale bar: 20 μm. (B) The length (left) and the number (right) of neurites quantified in GFP expressing cells. Each column in the right graph represents the number of neurites as indicated. (**P*<0.001, ***P*<0.0001, in comparison with the wild-type GFP control; ****P*<0.07 in comparison with the mutant GFP control).

and that its action is cell-autonomous in the granule cell, we hypothesized that Pax6 regulates transcription of cytoplasmic and/or transmembrane protein(s) implicated in cellular morphogenesis of granule cells during axon formation and migration.

We noticed that *Pax6* mutant cells had multipolar processes with occasional bifurcated branches or lamellipodia (Fig. 7A,B). Growth cones at the tips of axons were also found to be larger in the mutant cells compared to the wild-type (Fig. 7C-G). Double-immunofluorescence staining revealed entry of actin and microtubule networks into those growth cones (Fig. 7E,F). These phenotypes were reminiscent of those seen following treatment with an inhibitor of p160 ROCK, a Rho GTPase-associated kinase (Bito et al., 2000).

The above observation raised an intriguing possibility that *Pax6* might regulate the expression of factor(s) implicated in the Rho/ROCK pathway. To assess this possibility, we first examined initial outgrowth of axons in dissociated EGL cells (Fig. 8). By 20 hours after plating, most wild-type cells extruded bipolar neurites, presumably forming future parallel fiber axons (Fig. 8A,G). In contrast, a significant proportion of *Pax6* mutant cells possessed an increased number of processes (Fig. 8D,G). Differences in neurite lengths between wild-type and mutant cells were not prominent at 20 hours of culture. Wild-type cells treated with Y27632, a specific inhibitor of ROCK, exhibited multipolar morphology similar to *Pax6* mutant cells (Fig. 8B). The only noticeable difference in their phenotypes was a slight increase in axon length in Y27632-treated cells (Fig. 8H). Overexpression of a RhoA-inhibiting enzyme, C3, resulted in further enhancement of similar phenotypic changes (Fig. 8C). We also tested modulators of other small GTPases, including dominant-negative and constitutively-active forms of Cdc42 and Rac1, but they exhibited phenotypes apparently distinct from *Pax6* mutant cells (data not shown). As these observations suggested that *Pax6* might be involved in the Rho/ROCK pathway, we blocked the Rho/ROCK pathway in *Pax6* mutant cells by treatment with Y27632 or by misexpression of C3, and quantified the number and the length of neurites in comparison with untreated mutant cells. We hypothesized that if the phenotype of *Pax6* mutant cells was caused by loss of expression of factor(s) implicated in the Rho/ROCK pathway, there should be little additional change in the phenotypes of *Pax6*-deficiency by treatment with Y27632 or C3. However, the effects of Y27632 and C3 were additive in the *Pax6* mutant cells; the number and the length of neurites were significantly augmented by treatment with Y27632 or C3 (Fig. 8D-H). Furthermore, misexpression of the constitutively-active form

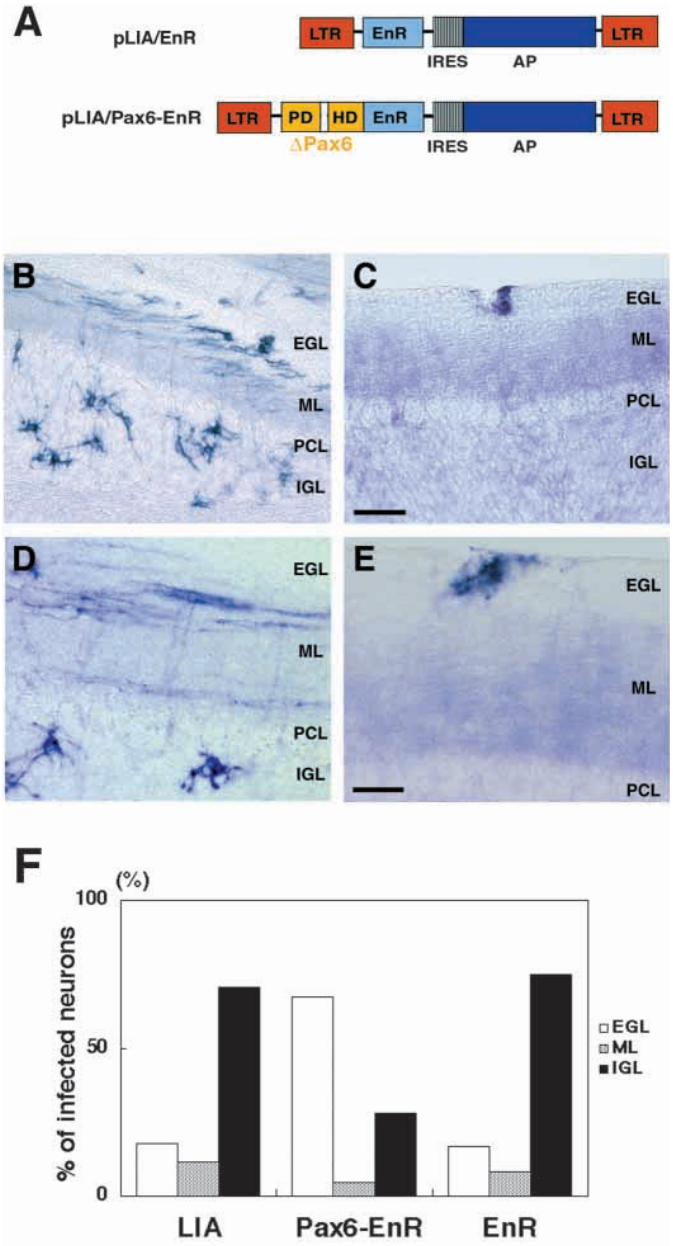

Fig. 6. Altered morphology and behavior of EGL cells transduced by dominant negative Pax6 virus. (A) Viral constructs used for expressing Pax6-EnR and EnR. Infected cells express a marker gene, alkaline phosphatase (AP), through an IRES sequence. HD, homeodomain; PD, paired domain. (B,D) Cells infected with EnR viruses appear in the IGL and display a granule cell morphology with small, round soma, parallel fibers and claw-like dendrites. (C,E) The EGL cells infected with Pax6-EnR viruses fail to migrate and cluster around the injection site. Neither parallel fibers nor mature granule cells in the IGL are observed. Scale bars: 40 μm in B,C; 20 mm in D,E. (F) The percentages of infected cells found in each layer.

of ROCK (Delta 3) had a comparable inhibitory effect on neurite formation in both wild-type and mutant cells (data not shown). These results suggested that the phenotypes caused by the absence of *Pax6* function was unlikely to be mediated by a modification of endogenous ROCK activity.

DISCUSSION

In this study, we have demonstrated that *Pax6* controls a genetic program involved in the polarization of cerebellar granule cells. In the *Pax6* mutant rat $rSey^2/rSey^2$, granule cells displayed severe morphological abnormalities including multipolar neurites and random migration, despite apparently normal expression of a series of granule cell axonal differentiation markers. These results suggest that *Pax6* acts at the level of cellular morphogenesis and migration rather than in regulation of the early steps of granule cell determination or differentiation. We also showed that cytoskeletal dynamics of mutant granule cells were apparently disorganized in a manner reminiscent of the inhibition of the ROCK pathway. To our knowledge, this is the first indication that *Pax6* functions as an intrinsic factor regulating neuronal morphogenesis and migration via cytoskeletal control.

Cell-autonomous function of *Pax6* during parallel fiber formation and tangential migration of granule cells

Pax6 mutant animals show a wide variety of neurological abnormalities in migration and axonal pathfinding of CNS neurons. However, most of the phenotypes characterized so far result from indirect effects of *Pax6* mutation. In sharp contrast, granule cells require the intrinsic activity of *Pax6* to properly form bipolar axons and for subsequent cell body migration, implicating Pax6-involvement in the transcriptional control required for polarization of axons. Disrupted formation of long bipolar neurites in mutant cells was rescued by forced expression of *Pax6*, but not by co-culturing with wild-type cells, indicating cell-autonomy of *Pax6* function during granule cell morphogenesis. Combinatorial expression of different markers for granule cells and parallel fiber axons ensured that *Pax6* mutant EGL cells were competent to differentiate as granule cells and to form parallel fiber axons. It is thus plausible that *Pax6* is involved in polar elongation of axons after the initial stage of their formation.

Another striking feature of *Pax6* mutant EGL cells is their unsteady zigzag migration path in culture. While wild-type EGL cells elongated long leading processes along preexisting radial axons, *Pax6* mutant cells extended short leading processes in random orientations that often detached from the axons, as visualized by immunofluorescence against MAP2 and by TEM studies. Our co-culture experiments demonstrated that this disorganized migration of *Pax6* mutant cells was not due to the absence of a radial neurite scaffold, but rather to a cell-autonomous defect of migrating cells. Thus, besides its role in axon elongation, *Pax6* might also be involved in regulation of tangential migration of granule cells guided by leading processes that contact with preformed axon fibers. In contrast to the mutant cells in culture, the EGL cells that misexpress a dominant-negative *Pax6* failed to move away from the site of their birth in developing cerebella. The appearance of the thickened EGL of mutant animals also suggests that tangential migration of premigratory EGL cells are disturbed in the absence of *Pax6* function. This is not surprising if one considers that tangential migration of postmitotic EGL cells is guided by leading processes via contact-mediated association with pre-existing parallel fibers. Hence, densely packed EGL cells might offer massive

resistance to the passage of *Pax6*-deficient cells that randomly move on the free surface of a culture dish.

Which step of parallel fiber formation – formation of the bipolar leading and trailing processes, tangential migration, or axon elongation – does *Pax6* specifically regulate? As the leading and trailing processes of bipolar EGL cells are later transformed into parallel fiber axons (Ono et al., 1994), it is difficult to draw a sharp distinction between these continuous steps in granule cell morphogenesis. From our data, it is likely that *Pax6* function is involved in axon elongation as well as during the initial outgrowth of bipolar neurites, as expression of *Pax6* after 1 DIV was sufficient to rescue attenuated elongation of bipolar neurites in mutant cells (Fig. 5). Thus, the cell-autonomous function of *Pax6* may be involved in sustaining the formation of bipolar processes that guide tangential migration and later elongate to form parallel fiber axons.

Cellular mechanisms downstream of *Pax6* function

We also searched for the cellular mechanisms regulating granule cell morphogenesis impaired in *Pax6* mutant cells. Formation of multiple axonal processes, abnormal lamellipodia and increase in the growth cone size in mutant cells strongly suggest an important role for *Pax6* in the control of cytoskeletal dynamics during neurite formation. Apparent similarities in the phenotypes of *Pax6* mutant cells with those evoked by inhibition of the Rho/ROCK activities prompted us to examine a functional interaction of *Pax6* and the Rho/ROCK pathway. Quantitative analysis of the action of Y-27632 on *Pax6* mutant cells excluded direct involvement of *Pax6* in the ROCK pathway. In other words, it is unlikely that *Pax6* regulates expression of signaling molecule(s) in direct association with ROCK. Some differences in the phenotypes of mutant cells and ROCK-inhibited cells were observed: a mild increase in axon length, presumably owing to early initiation of axon outgrowth, was seen in Y27632-treated cells but not in *Pax6*-mutant cells (Fig. 8). In fact, unlike Y27632 treatment, initiation of neurite formation was not advanced in mutant cells (data not shown). Nevertheless, several common morphological features between *Pax6*- and ROCK-deficient cells suggested that *Pax6* might regulate cytoskeletal dynamics via a mechanism closely related to the ROCK pathway. One possibility to be tested in future studies is that *Pax6* may be involved in a step maintaining neuronal polarity downstream of ROCK-mediated initial polarization of granule cells. The enhanced phenotypes induced by the Rho-inhibiting enzyme C3 are consistent with the idea that multiple co-existing Rho-dependent mechanisms regulate actin and/or other cytosketetal dynamics (Kaibuchi et al., 1999; Bito et al., 2000; Bradke and Dotti, 2000). C3 expression yielded alterations in the number and the length of axons of wild-type and mutant cells to a similar plateau, implying that loss of *Pax6* function might cause inactivation of a ROCK-independent Rho pathway. Alternatively, *Pax6* might be involved in a cascade independent of Rho/ROCK activity, as we cannot rule out that phenotypes evaluated by the parameters we used in this study were saturated in C3-expressing cells.

It is noteworthy that in culture, *Pax6* mutant neocortical radial glia and cerebellar granule cells exhibit similar morphological abnormalities (Götz et al., 1998): they form multipolar short processes instead of long bipolar processes of

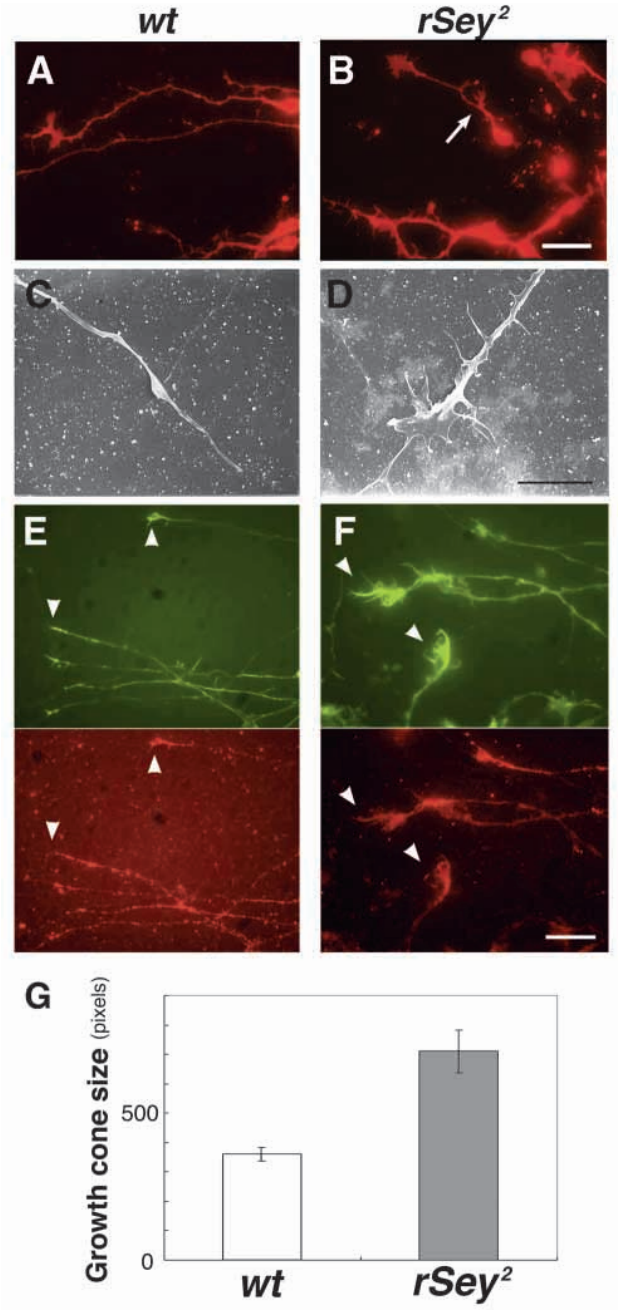

Fig. 7. Aberrant formation of cytoskeletal structures in *Pax6* mutant (*rSey²/rSey²*) EGL cells. (A,B) PKH26-labeled cells emigrating from a microexplant of E21 EGL observed at 1 DIV. Wild-type cells (A) have long straight neurites, while mutant cells (B) protrude short neurites, occasionally bifurcated and/or extruding lamellipodia in the midst of the shafts (arrow). (C,D) Scanning electron micrographs of microexplant cultures (3 DIV). Wild-type cells (C) possess thin growth cones at the tip, most of which simply taper off. *Pax6* mutant cells (D) expand large growth cones with massive lamellipodia. (E,F) Distribution of F-actin (green) and microtubules (red) in growth cones. In comparison with wild type (E), an excess amount of F-actin accumulates in the large growth cones of *Pax6* mutant EGL cells, accompanied by invasion of microtubules (F). (G) Quantification of growth cone size. Live cells labeled with PKH26 were observed at 1 DIV. The growth cone area was measured as the number of pixels in the graphic image. Data are indicated as mean±s.e.m. ($P<0.005$). Scale bars: 10 μm.

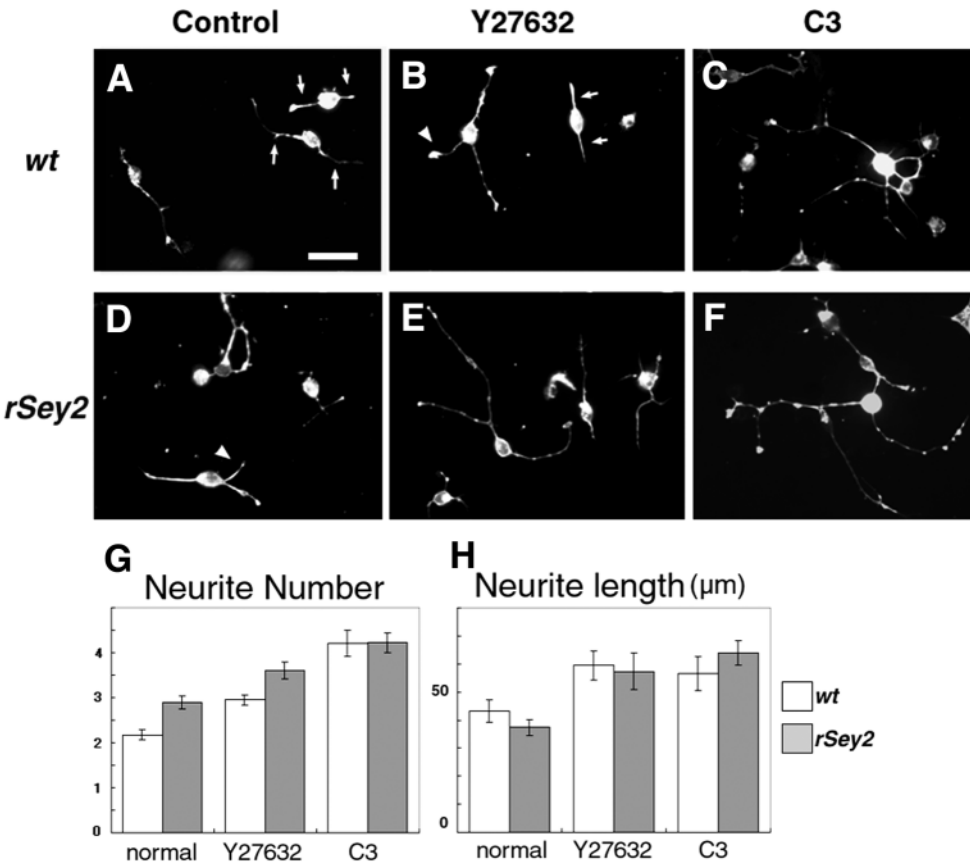

Fig. 8. Functional interaction of *Pax6* with the Rho/ROCK pathway in axonogenesis of the granule cell. (A-F) Morphology of neurons from wild-type (A-C) and *Pax6* mutant (D-F) EGLs. Dissociated EGL cells were labeled with PKH26 and cultured at a low density for 20 hours. Most wild-type cells (A) have bipolar processes (arrows), whereas excess neurites are present in *Pax6* mutant cells (D) as well as Y-27632-treated cells (B) (arrowheads). See text for details. Scale bar: 20 μm. (G,H) Quantitative analyses of the number (G) and length (H) of axons induced by Y-27632-treatment or by C3 misexpression. Data are indicated as mean±s.e.m. $P<0.001$ in comparison with the respective untreated controls for wild-type cells (white bars) and mutant cells (gray bars).

wild-type cells. This raises an intriguing possibility that *Pax6* might have a general role in regulating cytoskeletal dynamics during polarization of neural cells in the CNS. *Pax6* may activate transcription of the genes required for organization of cytoskeletal proteins in granule cells, which should act independently of the ROCK pathway. Identification of downstream target genes for *Pax6* is in progress to reveal the molecular cascades that control the dynamic change of granule cell polarity during development.

Contribution of Pax6 in other aspects of cerebellar development

Pax6 expression is first detected in the EGL stem cells in the upper rhombic lip at as early as E14.5 in normal rat embryos (K. K. and M. K., unpublished). The EGL stem cells move rostrally from the upper rhombic lip along the surface of the cerebellar primordium to form the EGL by E19 in rodents. This raises the possibility that *Pax6* is involved in the early phase of cerebellar development, including migration of the stem cells to populate the EGL. Previous studies have indeed shown that a subset of EGL cells is mislocated in the inferior colliculus in the *Pax6* mutant mouse *Sey*/*Sey* (Engelkamp et al., 1999). This ectopic extension of the EGL may be the result of loss of *Unc5h3* expression in the *Sey/Sey* mouse. However, in the rat $rSey^2/rSey^2$ mutants, we found no difference in the level of expression of *netrin* and its receptors, including *Dcc*, *Unc5hs* and *neogenin*, in the EGL (data not shown). Consistently, the rostral migration of EGL stem cells appeared normal in rats, suggesting that neither loss of *Unc5h3* expression nor mislocation of EGL cells necessarily occur in the context of *Pax6* deficiency. That the EGL was completely covered by granule cells in *Pax6* mutant animals supports the notion that the initial migration of EGL stem cells does not require *Pax6* function. Histological analysis could distinguish rostral migration of the EGL stem cells from tangential migration of premigratory EGL cells, in that the former is not guided by leading processes but resembles passive dispersal of round cells (Ryder and Cepko, 1994; Altman and Bayer, 1997; Komuro et al., 2001). It is intriguing that leading process-guided migration of lower rhombic lip cells to form precerebellar nuclei is also disrupted in *Pax6* mutant animals (Engelkamp et al., 1999; Yee et al., 1999). Thus, the ability of *Pax6* to regulate migration may be a mechanism common to neurons that use leading processes in the cerebellar system.

What is the role of early expression of *Pax6* in the upper rhombic lip cells? Besides abnormal behavior of EGL cells, multiple morphological defects are observed in *Pax6* mutant cerebellum, including mediolateral regionalization of the cerebellar primordium. Early expression of *Pax6* might regulate these aspects independently of its action on postmitotic EGL cells.

Concluding remarks

Pax6 plays critical roles in numerous aspects of early patterning and cell-type specification in the CNS. Our present report pinpoints a novel function of *Pax6* in the cell-autonomous control of cytoskeletal networks during the polarization of the CNS neuron. As could be speculated from its pleiotropic actions during development, downstream targets of *Pax6* might well be context dependent within individual *Pax6*-expressing cells. It would thus be necessary to identify the specific target genes in the granule cell to clarify the molecular mechanisms regulating formation of their bipolar axons. Further studies will be needed to understand how widely

this *Pax6*-dependent mechanism is used in various cell types during polarization in the developing CNS.

We thank L. Cai, T. Furukawa and C. Cepko for technical advice, I. Nagata for helpful discussion, Y. Yoneyama, T. Nagase and N. Takashima for technical assistance, and R. T. Yu for critical reading of the manuscript. We also thank S. Narumiya for C3-GFP and ROCK-Delta3, G. Nolan for Phoenix cell line, P. Gruss for Pax6 cDNA, J. Aruga for an anti-Zic1 antibody, M. Kunimoto for an anti-Ankyrin$_B$ antibody and A. Yoshimura (Welfide) for Y27632. This work was supported by Grants in Aid from the Ministry of Education, Science, Sports, and Culture of Japan to M. K., K. O., H. B. and N. O., grants from CREST to M. K. and T. H., and grants from Uehara Memorial Fellowship and Naito Memorial Bioscience Fellowship to M. K.

REFERENCES

Albertinazzi, C., Cattelino, A. and de Curtis, I. (1999). Rac GTPases localize at sites of actin reorganization during dynamic remodeling of the cytoskeleton of normal embryonic fibroblasts. *J. Cell Sci.* **112**, 3821-3831.

Altman, J. and Bayer, S. A. (1997). *Development of The Cerebellar System In Relation to Its Evolution, Structure, and Functions*. New York: CRC Press.

Aruga, J., Yokota, N., Hashimoto, M., Furuichi, T., Fukuda, M. and Mikoshiba, K. (1994). A novel zinc finger protein, zic, is involved in neurogenesis, especially in the cell lineage of cerebellar granule cells. *J. Neurochem.* **63**, 1880-1890.

Bhatt, R. S., Tomoda, T., Fang, Y. and Hatten, M. E. (2000). Discoidin domain receptor 1 functions in axon extension of cerebellar granule neurons. *Genes Dev.* **14**, 2216-2228.

Bito, H., Furuyashiki, T., Ishihara, H., Shibasaki, Y., Ohashi, K., Mizuno, K., Maekawa, M., Ishizaki, T. and Narumiya, S. (2000). A critical role for a Rho-associated kinase, p160ROCK, in determining axon outgrowth in mammalian CNS neurons. *Neuron* **26**, 431-4341.

Bradke, F. and Dotti, C. G. (1999). The role of local actin instability in axon formation. *Science* **283**, 1931-1934.

Bradke, F. and Dotti, C. G. (2000). Establishment of neuronal polarity: lessons from cultured hippocampal neurons. *Curr. Opin. Neurobiol.* **10**, 574-581.

Burrill, J. D., Moran, L., Goulding, M. D. and Saueressig, H. (1997). PAX2 is expressed in multiple spinal cord interneurons, including a population of EN1+ interneurons that require PAX6 for their development. *Development* **124**, 4493-4503.

Caric, D., Gooday, D., Hill, R. E., McConnell, S. K. and Price, D. J. (1997). Determination of the migratory capacity of embryonic cortical cells lacking the transcription factor Pax-6. *Development* **124**, 5087-5096.

Cepko, C. L., Ryder, E., Austin, C., Golden, J., Fields-Berry, S. and Lin, J. (1998). Lineage analysis using retroviral vectors. *Methods* **14**, 393-406.

Dahmane, N. and Ruiz-i-Altaba, A. (1999). Sonic hedgehog regulates the growth and patterning of the cerebellum. *Development* **126**, 3089-3100.

Engelkamp, D., Rashbass, P., Seawright, A. and van Heyningen, V. (1999). Role of Pax6 in development of the cerebellar system. *Development* **126**, 3585-3596.

Ericson, J., Rashbass, P., Schedl, A., Brenner-Morton, S., Kawakami, A., van Heyningen, V., Jessell, T. M. and Briscoe, J. (1997). Pax6 controls progenitor cell identity and neuronal fate in response to graded Shh signaling. *Cell* **90**, 169-180.

Furley, A. J., Morton, S. B., Manalo, D., Karagogeos, D., Dodd, J. and Jessell, T. M. (1990). The axonal glycoprotein TAG-1 is an immunoglobulin superfamily member with neurite outgrowth-promoting activity. *Cell* **61**, 157-170.

Furukawa, T., Morrow, E. M. and Cepko, C. L. (1997). Crx, a novel otx-like homeobox gene, shows photoreceptor-specific expression and regulates photoreceptor differentiation. *Cell* **91**, 531-541.

Goodhill, G. J. (1998). Mathematical guidance for axons. *Trends Neurosci.* **21**, 226-231.

Goodman, C. S. and Shatz, C. J. (1993). Developmental mechanisms that generate precise patterns of neuronal connectivity. *Cell* **72 Suppl.**, 77-98.

Götz, M., Stoykova, A. and Gruss, P. (1998). Pax6 controls radial glia differentiation in the cerebral cortex. *Neuron* **21**, 1031-1044.

Hatten, M. E. and Heintz, N. (1995). Mechanisms of neural patterning and specification in the developing cerebellum. *Annu. Rev. Neurosci.* **18**, 385-408.

Inoue, T., Nakamura, S. and Osumi, N. (2000). Fate mapping of the mouse prosencephalic neural plate. *Dev. Biol.* **219**, 373-383.

Ishizaki, T., Naito, M., Fujisawa, K., Maekawa, M., Watanabe, N., Saito, Y. and Narumiya, S. (1997). p160ROCK, a Rho-associated coiled-coil forming protein kinase, works downstream of Rho and induces focal adhesions. *FEBS Lett.* **404**, 118-124.

Kaibuchi, K., Kuroda, S. and Amano, M. (1999). Regulation of the cytoskeleton and cell adhesion by the Rho family GTPases in mammalian cells. *Annu. Rev. Biochem.* **68**, 459-486.

Katsumoto, T., Naguro, T., Iino, A. and Takagi, A. (1981). The effect of tannic acid on the preservation of tissue culture cells for scanning electron microscopy. *J. Electron Microsc.* **30**, 177-182.

Kawano, H., Fukuda, T., Kubo, K., Horie, M., Uyemura, K., Takeuchi, K., Osumi, N., Eto, K. and Kawamura, K. (1999). Pax-6 is required for thalamocortical pathway formation in fetal rats. *J. Comp. Neurol.* **408**, 147-160.

Komuro, H., Yacubova, E. and Rakic, P. (2001). Mode and tempo of tangential cell migration in the cerebellar external granular layer. *J. Neurosci.* **21**, 527-540.

Kunimoto, M. (1995). A neuron-specific isoform of brain ankyrin, 440-kD ankyrinB, is targeted to the axons of rat cerebellar neurons. *J. Cell Biol.* **131**, 1821-1829.

Lin, J. C. and Cepko, C. L. (1998). Granule cell raphes and parasagittal domains of Purkinje cells: complementary patterns in the developing chick cerebellum. *J. Neurosci.* **18**, 9342-9353.

Luo, L., Hensch, T. K., Ackerman, L., Barbel, S., Jan, L. Y. and Jan, Y. N. (1996). Differential effects of the Rac GTPase on Purkinje cell axons and dendritic trunks and spines. *Nature* **379**, 837-840.

Mastick, G. S., Davis, N. M., Andrew, G. L. and Easter, S. S., Jr (1997). Pax-6 functions in boundary formation and axon guidance in the embryonic mouse forebrain. *Development* **124**, 1985-1997.

Matsunaga, E., Araki, I. and Nakamura, H. (2000). Pax6 defines the di-mesencephalic boundary by repressing En1 and Pax2. *Development* **127**, 2357-2365.

Matsuo, T., Osumi-Yamashita, N., Noji, S., Ohuchi, H., Koyama, E., Myokai, F., Matsuo, N., Taniguchi, S., Doi, H., Iseki, S. et al. (1993). A mutation in the Pax-6 gene in rat small eye is associated with impaired migration of midbrain crest cells. *Nat. Genet.* **3**, 299-304.

Nagata, I. and Nakatsuji, N. (1990). Granule cell behavior on laminin in cerebellar microexplant cultures. *Dev. Brain Res.* **52**, 63-73.

Nagata, I. and Nakatsuji, N. (1991). Rodent CNS neuroblasts exhibit both perpendicular and parallel contact guidance on the aligned parallel neurite bundle. *Development* **112**, 581-590.

Nagata, I. and Nakatsuji, N. (1994). Migration behavior of granule cell neurons in cerebellar cultures. I. A PKH26 labeling study in microexplant and organotypic cultures. *Dev. Growth Differ.* **36**, 19-27.

Nakayama, A. Y., Harms, M. B. and Luo, L. (2000). Small GTPases Rac and Rho in the maintenance of dendritic spines and branches in hippocampal pyramidal neurons. *J. Neurosci.* **20**, 5329-5338.

Ono, K., Nakatsuji, N. and Nagata, I. (1994). Migration behavior of granule cell neurons in cerebellar cultures. II. An electron microscopy study. *Dev. Growth Differ.* **36**, 29-38.

Osumi, N., Hirota, A., Ohuchi, H., Nakafuku, M., Iimura, T., Kuratani, S., Fujiwara, M., Noji, S. and Eto, K. (1997). Pax-6 is involved in the specification of hindbrain motor neuron subtype. *Development* **124**, 2961-2972.

Powell, S. K., Rivas, R. J., Rodriguez-Boulan, E. and Hatten, M. E. (1997). Development of polarity in cerebellar granule neurons. *J. Neurobiol.* **32**, 223-236.

Pratt, T., Vitalis, T., Warren, N., Edgar, J. M., Mason, J. O. and Price, D. J. (2000). A role for pax6 in the normal development of dorsal thalamus and its cortical connections. *Development* **127**, 5167-5178.

Ryder, E. F. and Cepko, C. L. (1994). Migration patterns of clonally related granule cells and their progenitors in the developing chick cerebellum. *Neuron* **12**, 1011-1028.

Schmahl, W., Knoedlseder, M., Favor, J. and Davidson, D. (1993). Defects of neuronal migration and the pathogenesis of cortical malformations are associated with Small eye (Sey) in the mouse, a point mutation at the Pax-6-locus. *Acta Neuropathol.* **86**, 126-135.

Steven, R., Kubiseski, T. J., Zheng, H., Kulkarni, S., Mancillas, J., Ruiz Morales, A., Hogue, C. W., Pawson, T. and Culotti, J. (1998). UNC-73

activates the Rac GTPase and is required for cell and growth cone migrations in C. elegans. *Cell* **92**, 785-795.

Stoykova, A. and Gruss, P. (1994). Roles of Pax-genes in developing and adult brain as suggested by expression patterns. *J. Neurosci.* **14**, 1395-1412.

Stoykova, A., Treichel, D., Hallonet, M. and Gruss, P. (2000). Pax6 modulates the dorsoventral patterning of the mammalian telencephalon. *J. Neurosci.* **20**, 8042-8050.

Threadgill, R., Bobb, K. and Ghosh, A. (1997). Regulation of dendritic growth and remodeling by Rho, Rac, and Cdc42. *Neuron* **19**, 625-634.

Tomoda, T., Bhatt, R. S., Kuroyanagi, H., Shirasawa, T. and Hatten, M. E. (1999). A mouse serine/threonine kinase homologous to C. elegans UNC51 functions in parallel fiber formation of cerebellar granule neurons. *Neuron* **24**, 833-846.

Toresson, H., Potter, S. S. and Campbell, K. (2000). Genetic control of dorsal-ventral identity in the telencephalon: opposing roles for pax6 and gsh2. *Development* **127**, 4361-4371.

Trenkner, E., Smith, D. and Segil, N. (1984). Is cerebellar granule cell migration regulated by an internal clock? *J. Neurosci.* **4**, 2850-2855.

Vitalis, T., Cases, O., Engelkamp, D., Verney, C. and Price, D. J. (2000). Defect of tyrosine hydroxylase-immunoreactive neurons in the brains of mice lacking the transcription factor Pax6. *J. Neurosci.* **20**, 6501-6516.

Watanabe, N., Kato, T., Fujita, A., Ishizaki, T. and Narumiya, S. (1999). Cooperation between mDia1 and ROCK in Rho-induced actin reorganization. *Nat. Cell Biol.* **1**, 136-143.

Wechsler-Reya, R. J. and Scott, M. P. (1999). Control of neuronal precursor proliferation in the cerebellum by Sonic Hedgehog. *Neuron* **22**, 103-114.

Yamamoto, M., Hassinger, L. and Crandall, J. E. (1990). Ultrastructural localization of stage-specific neurite-associated proteins in the developing rat cerebral and cerebellar cortices. *J. Neurocytol.* **19**, 619-627.

Yee, K. T., Simon, H. H., Tessier-Lavigne, M. and O'Leary, D. M. (1999). Extension of long leading processes and neuronal migration in the mammalian brain directed by the chemoattractant netrin-1. *Neuron* **24**, 607-622.

Yun, K., Potter, S. and Rubenstein, J. L. (2001). Gsh2 and Pax6 play complementary roles in dorsoventral patterning of the mammalian telencephalon. *Development* **128**, 193-205.

Zhang, L. and Goldman, J. E. (1996). Generation of cerebellar interneurons from dividing progenitors in white matter. *Neuron* **16**, 47-54.

Zipkin, I. D., Kindt, R. M. and Kenyon, C. J. (1997). Role of a new Rho family member in cell migration and axon guidance in C. elegans. *Cell* **90**, 883-894.